ISSN: 0369-8963

Multi-point Vibration Measurement in an Agriculture Tractor Mudguard using Finite Difference and Up-sampled Cross-Correlation Algorithm

R.GANESAN[1, 2*], G.SANKARANARAYANAN[1], M. PRADEEP KUMAR[3], V.K. BUPESH RAJA[1]

[1] Research Scholar, Research Supervisor, Professor, Department of Mechanical Engineering, Sathyabama Institute of Science and Technology, Chennai, 600119, India*
[2]Department of Mechanical Engineering, Sree Sastha Institute of Engineering and Technology, Chennai, India.
[3]Professor, Department of Mechanical Engineering, CEGC, Anna University, Chennai, 600025, India

** Corresponding author: R.Ganesan*

Abstract:

This experiment proposes the measurement of vibration at several points of a machine part using a machine vision system and compares the results with those measured using the conventional vibration measurement technique. Vibration measurements of two closer points on the part of the machine by the vibration sensors may have errors depending on the sensitivity of the vibration sensors. The acceleration sensors, which are fixed at a closer distance, may sense the vibration wrongly because of the continuity of structures. Vibration calculated by machine vision is a non-contact measurement process, so the sensitivity of the sensor does not become a factor here. Like other machine vision systems, the function includes image capturing, image pre-processing, image processing, and data recovery from the images. The main difference between this study and the others is that the camera calibration has been conveniently modified. The camera calibration is made easy by a paper sticker with well-known dimensions. The real-world dimensions of the paper sticker and the dimension of the image are brought to real-world dimensions. The coloured dot placed on this paper sticker has been treated as a target. The structure of the machine undergoes microscopic displacement due to vibrations. By calculating these displacements, the vibrations are calculated using the appropriate mathematical formulas.

Keywords: *Machine vision; Condition monitoring; Industry 4.0; Multipoint vibration measurement.*

INTRODUCTION

Machine vibration analysis is critical for monitoring and maintaining machine health. Vibration analysis can determine a machine's present status. It can predict machine maintenance via condition monitoring. This is a method of anticipating and correcting errors. Machine failure that occurs unexpectedly or without warning is a waste of both money and time. The vibration analysis method is a straightforward way to anticipate a machine's health. When the machine's internal components fail, the state of the machine can be established by analysing these fluctuations in the machine's vibration. Someone can do manual repair detection by frequency variation or by using an automated technique. Modern computer programming and sensor technology make automated condition monitoring much easier. Investing in such technologies will allow you to increase your profits while avoiding the costs of spare parts, maintenance, and time loss. Continuous vibration monitoring contributes to improving machine performance. It is possible to record continuous vibration measurements and transfer them to different systems, such as computers, cell phones, and so on, to monitor the current operations of the machine using advanced vibration analysis methods. [1-5]

The sensitivity of a piezoelectric accelerometer sensor changes when its exposed components to ambient temperature. Accelerators typically carry heat up to 250 degrees Celsius. When the accelerometer is subjected to elevated temperatures, its parts undergo permanent deformation. It is therefore advisable to use special accelerometers that can withstand high temperatures above 250 degrees Celsius. Special accelerometer sensors can operate from minus 196 degrees Celsius to 480 degrees Celsius. Triboelectric noise, and ground loop noise on the cable to which the accelerometer attached, may affect the sensor's sensitivity. It subjected the base of the accelerometer sensor to deformation because of the accelerometer sensor mounting on the surface of the machine using several methods and the vibration measurement captured from it may change. Nuclear radiation above

 https://doi.org/10.37896/pd91.4/91484

ISSN: 0369-8963

20 kGy affects the sensitivity of the accelerometer. Moisture and oil buildup on the top of the machine can affect the performance of the accelerometer. [6]

The mission vision system plays an important role in displacement measurements. Vision-based displacement measurement methods are superior to conventional displacement measurement methods in factors such as instrumentation cost, installation cost, and measurement capacity make the vision-based displacement measurement methods superior to conventional displacement measurement methods.[7]. Vision-based displacement monitoring systems Setting up one or more cameras in a stable area, gazing at the ‘target’ housed in a structure, and deriving structural displacement through target tracking is required when using a vision-based system for structural displacement monitoring. The "target" in this case could be something like a pre-installed marker, an LED bulb, or a flat panel with a specific pattern, or it could be a part of the structure, like bolts or holes.

The camera, lens, laptop or portable computer with the video-processing package, and other peripherals, such as a tripod, make up the gear. The image processing software is very important. It collects video frames that cover the target area, keeps track of where the target is in each image frame, and finally turns the location of the target in an image into a record of structural movement over time.

Systems for getting metric information from pictures or videos include digital image correlation (DIC) [8, 9, 10], photogrammetric approaches [11], and motion capture systems (MCS) [12, 13]. In experimental solid mechanics, DIC is a measuring method for extracting full-field displacements or stresses of a member surface [10, 14, and 15]. Photogrammetry, which was first used to create topographic maps [16], has now been broadened to incorporate bridge deflection monitoring [17]. Motion capture systems (MCS) are often used to capture the motions of a multi-jointed skeletal structure with a large degree of freedom (e.g., human bodies) [18].

It built the projection link between the 3D structural points in the structural coordinate system and the associated 2D points in the picture plane during camera calibration. Given the target positions in the picture, the calculated projection transformation might retrieve the true locations of targets in the structure. Wide-angle lenses are used in consumer cameras and smartphone cameras to enhance the field of vision [19], resulting in distorted pictures, particularly in the corners of the frame. The distortion correction step is not required for cameras with lenses that produce no visible lens distortion. For monitoring, it makes sense that the target area should be close to the centre of the field of vision [20], where lens distortion is less.

The easiest projection conversion is a scale factor, which presupposes that all projected points have the same depth of field or that the optical axis is perpendicular to one structural plane [20-21]. Given the picture position of an object (output of target tracking) and the projection transformation relationship, structural displacement might be calculated from the change in structural coordinates (output of camera calibration). [22]

The fundamental benefit of vibration analysis using a high-speed camera is the potential to collect more data about the events noticed during vibration propagation and their influence on other mechanical equipment with no extra classification, analysis, or interpretation. The rapid development of image recording devices, microprocessors, next-generation computer memory, and image identification and analysis algorithms allows us to forecast that the use of high-speed cameras for vibration analysis will become more widespread. [23]

Finally, while there are more accurate technologies available, they are confined to specific point measurements (accelerometer, laser vibrometer) or vast area integration (microphone). As a result, our suggestion might be a beneficial addition to these gadgets, providing important information regarding complicated issues. [24–25]

 https://doi.org/10.37896/pd91.4/91484

ISSN: 0369-8963

The location of the sensor fitting is important in designing an acceptable condition monitoring system. The stability and reliability of the information obtained depend entirely on the location where the sensor is mounted. This research paper examines the relationship between faults in the gearbox and sensor fitting locations. Better valid information can be obtained by fitting sensors in the right place. This allows the machine to be monitored by alternating methods, such as vibration and sound emission monitoring. The test work is outlined to assess the ideal sensors' position for recognizing issues within the gearbox framework. It worked the gearbox under solid and undesirable conditions with shifting levels of successful speed and stack, utilising a full factorial exploratory plan strategy. The ghostly kurtosis has been executed as a tangible inclusion by computing the kurtosis for the extent of recurrence components in a time recurrence graph. The results of this study have showed that the implemented approach may be an appropriate strategy for giving a better understanding of acoustic emanation and vibration signals to move forward the unwavering quality and the capability of condition motioning systems.

It investigated a novel application of the early development strategy for sensor arrangement and signal conditioning changes in gearbox systems using vibration and acoustic sensors. It found the strategy to be probably important for recognising the perfect position for the sensors to check the gearbox system with the most reasonable signal conditioning. It found that the recommended strategy can demonstrate the sensitive position of the sensors among the first chosen ones to ensure good quality of signals and a consistent condition monitoring system. [26]

Convolutional neural networks (CNNs), a deep learning-based target tracking approach, are largely utilised in computer vision applications. Environmental variables (e.g., lighting conditions, shadows, partial occlusion, and other fluctuations) make it difficult for a vision system to establish a stable and accurate displacement measurement over time in field applications.

This paper presents a unique distraction-free target tracking strategy by combining a deep learning-based Siamese tracker with classic correlation-based template matching to tackle these issues. There are several different Siamese trackers for template matching, and this study uses the DaSiamRPN tracker linked with the UpdateNet for adaptive template updating, which is robust in tough settings over time. In contrast to template matching, the Siamese tracker includes a bounding-box regression layer to forecast target localization, which includes four regression coefficients, two-directional position translation, and bounding-box size scaling. Because the task of measuring structural displacement is based on quantifying image variants of the region of interest, a correction step is added to remove centroid deviation between both the template and the predicted bounding boxes caused by image size changes when using correlation-based template matching. The suggested technique is first validated in a lab test before being deployed in monitoring experiments on a short-span footbridge and a long-span road bridge, proving its ability to handle demanding conditions such as occlusion, lighting, and backdrop variations. [27]

The DaSiamRPN tracker, which is connected to the UpdateNet, was chosen for early template matching. This is because of the DaSiamRPN architecture's inclusion of a distractor-aware learning module and a local-to-global search area technique, which makes it robust in demanding conditions such as occlusion, light change, and other changes. To address the long-term monitoring need, it also incorporated the UpdateNet to develop an adaptive intended template updating approach. The DaSiamRPN and the UpdateNet's core ideas are briefly explained below, and it may find additional information in [28, 29].

To overcome the problem of standard structural measurements failing to recover higher-frequency vibration signals, this research presents an improved zero-mean normalisation sum of squared differences (ZNSSD) technique. A high-speed camera records the high-speed picture series of target vibration in the developed model. The ZNSSD template matching technique is then used to process the collected pictures on the computer with sub-pixel precision. In addition, the ZNSSD

 https://doi.org/10.37896/pd91.4/91484

ISSN: 0369-8963

template matching method based on the image pyramid (ZNSSD-P), a changed search technique, has been developed to decimate calculation time and boost efficiency. Then, to increase the effectiveness of the ZNSSD-P method, a jumping ZNSSD template matching algorithm based on the image pyramid (J-ZNSSD-P) is presented. The Grating Ruler Motion Platform and acoustic impediments have been used to capture vibration signals. The results showed that this vibration signal extraction technique offers great robustness and accuracy.

A correlation value is used by the ZNSSD method to describe the correlation between two pictures. This is a matching method used to locate distinct objects in a picture. The use of a high-speed camera to gather movies of vibrating objects can yield significant data, but typical image processing algorithms are slower than a camera. Because of this mismatch, the vibration frequency measuring method based on high-speed vision has poor actual results. This work proposes an enhanced ZNSSD template matching method to increase the speed and precision of the standard ZNSSD template matching technique. The simulation results demonstrate that the enhanced method's precision and speed are much better than the conventional approach. In addition, two tests were conducted in the laboratory and outdoors to verify the precision and performance of the improved ZNSSD algorithm in practice. The findings showed that the suggested method extracts vibrating signals with excellent precision and performance. [30]

This study proposes and illustrates a multipoint vibration sensing approach based on the solid-core photonic crystal fibre (SCPCF) modal interferometry concept for sensing the immediate frequency, magnitude, and phase of vibrations about each interferometer. Fabrication of fibre combinations with speciality waveguides, such as SCPCF, enables stimulation and recombination of waveguide modes, resulting in consistent interference spectra over the source spectrum. To detect vibrations at each site, identical fibre topologies concatenated with a fibre channel operate as independent interferometers. The SCPCF is superior to standard fibre because it has a superior steering mechanism and a high temperature tolerance built in.

To obtain the data of vibrations about every interferometer, the resulting signal is examined using basic computational approaches. A comparable device has been studied earlier, but for stationary mechanical strain rather than real-time dynamic sensing. The suggested method allows for real-time strain measurement at numerous sites. [31-34]

Damage must be thoroughly assessed for a structure to be used safely and a management strategy to be developed. Although many attempts have been made to evaluate a building’s vibration to estimate the amount of damage, the precision of the assessment is not significant enough. Therefore, it’s impossible to state that a damage assessment based on vibrations in a structure has not been placed on actual usage. We present a technique to assess the damage by assessing the acceleration of a structure at various sites and analysing the information using a Random Forest, a type of machine learning algorithm. To increase damage evaluation precision, the suggested technique employs the highest response acceleration, standard deviation, logarithmic decay rate, and natural frequency. Based on the findings of these various assessments, we suggest a three-step Random Forest technique for evaluating diverse damage kinds. The suggested method’s correctness is confirmed using cross-validation and a vibration experiment on a real-world damaged specimen. The distance between the two successive acceleration sensor mountings is 260 mm. [35]

The phase-based optical flow was used in this study to introduce a non-contact multi-point vibration monitoring technique. For complicated structural anomaly identification, the approach may provide a full-field vibration map. Unlike conventional multi-point approaches that rely on intensity level variations, our method does not require any surface preparation and can achieve sub-pixel precision even in an outdoor setting. A specific noise reduction approach is used to boost the SNR while preserving the local motion fluctuations at each pixel.

 https://doi.org/10.37896/pd91.4/91484

ISSN: 0369-8963

It can calculate the magnified frequency bands without human input, as in the original motion magnification approach, by combining the multi-point measured values with the Maximum Likelihood Estimation (MLE), which improves the efficiency of mode magnification on complicated structures. The suggested procedure is checked by doing an experiment in a lab and taking a measurement in the field.

There are various aspects of this approach that might be improved in future research: First, with the camera angle perpendicular to the target object, this research solely looks at in-plane displacement. The vibrating structure in practise comprises both in-plane and out-of-plane movement, which may be done by creating a three-dimensional vibration map. Second, the suggested approach calculates vibration displacements at the pixel level. Torsion and twist of the structure, which cause the consideration of the relative movements of various motion signals, are not considered. Third, because of the low signal-to-noise ratio (SNR), the vibration map is generated using just the strongest peaks. In the future, mode decomposition can create clean vibration maps for all recognised modes. [36]

PROPOSED COMPUTER VISION SYSTEMS

For calculating displacement, template matching is a fundamental component of machine vision technique. A template-matching method is said to be a good tool in many research papers. Two successive picture images may be compared with the next location of the point in the image of a full image using this template machine algorithm. [5, 37, 38]

Assume an image J, with an offset of x = (x_a, x_b) and a template S of dimension r_S x c_S. The fit error E(x) can be expressed.

$$Err(x) = \sum_{i==1}^{rT}\sum_{j=1}^{cT}\left(Sr_{i,j} - Jr_{xa+i,xb+j}\right)^2 = 0 \qquad \text{Eqn.1}$$

$$Err(x) = \sum_{k=1}^{rS}\sum_{l=1}^{cS}\left(Sr_{i,j}\right)^2 - 2\sum_{k=1}^{rT}\sum_{l=1}^{cT}\left(Sr_{i,j}Jr_{xa+i,xb+j}\right) + \sum_{k=1}^{rS}\sum_{l=1}^{cS}\left(Jr_{xa+i,xb+j}\right)^2 = 0 \qquad \text{Eqn.2}$$

$$\text{Corre}_T(x) = \sum_{k=1}^{rT}\sum_{l=1}^{cT}\left(Sr_{i,j}Jr_{xa+i,xb+j}\right) \qquad \text{Eqn.3}$$

Scaling Factor Determination

To figure out the scaling factor SF from structural displacement to picture motion, you could use one-dimensional correspondence or the distance between the camera and the target.

$SF = \frac{|M1N1|}{|MsNs|}$ …… Eqn 4

$SF = \frac{FL}{DIST}$ ……. …….. Eqn 5

Where and denote the established physical dimension on the structural surface and the corresponding image size of the projection in the image, respectively; and FL denotes the camera lens focal length in pixel units, and DIST denotes the distance between the camera optical centre and the structural surface plane. [21] When comparing pictures, ensure that they are the same size in real life. The scaling factor plays a major role. The scaling factor was set using a white paper sticker with a pre-defined real-world dimension, adhered to the item surface where the vibration was to be detected before recording the video picture in this novel approach. On the sticker, a colour shows the dots. The template algorithm analyses two images and calculates the difference between them. [5, 39-43]

 https://doi.org/10.37896/pd91.4/91484

ISSN: 0369-8963

Object Tracking using Template Matching through Up-Sampled Cross-Correlation Algorithm

Template matching algorithms are classified into numerous categories. The key template methods are up-sampled cross-correlation and normalised cross-correlation. [5]

$$\text{DFT(u,v)}= \sum_{x,y} \frac{f_{vf}(x,y)}{\sqrt{MN}} \exp\left[-i2\pi\left(\frac{ux}{M}+\frac{ux}{N}\right)\right] \quad \text{Eqn.6}$$

Equation (6) uses a matrix multiplication discrete Fourier transform (MM-DFT) in a block around the first peak of RFT to get cross-correlation at the subpixel level. This saves time and makes subpixel resolution possible.

Computation of Acceleration for Vibration Measurement using Finite Element Algorithm.

To measure the displacement levels detected by the template matching technique, such as velocity measurements and acceleration measurements, were determined using template matching and a finite element algorithm. In addition to the current measurements, the aspiration measurements should be compared with the relationship measurements made by the acceleration sensor.

Velocity

$$V_{xj}=\left(\frac{(X(j+1)-X(j-1))}{2\times\nabla t}\right) \quad \text{Eqn.7}$$

$$V_{yj}=\left(\frac{(Y(j+1)-Y(j-1))}{2\times\nabla t}\right) \quad \text{Eqn.8}$$

Acceleration

$$aXj=\frac{(2\times X(j+2)-X(j+1)-2\times X(j)-X(j-1)+2\times X(j-2))}{(7\times\nabla t^2)} \quad \text{Eqn.9}$$

$$aYj=\frac{(2\times Y(j+2)-Y(j+1)-2\times Y(j)-Y(j-1)+2\times Y(j-2))}{(7\times\nabla t^2)} \quad \text{Eqn.10}$$

Field Tests- Experiment Setup

Experimental Model

An agricultural tractor, model TAFE 4410, was used as a test subject.Engine power: 32.8 kW, transmission: manual, wheelbase: 184 cm, weight: 1999 kg.

Camera

The Canon EOS 5D Mark II DSLR with 21.1 Megapixels, Movie Resolution: 1920 x 1080, 640 x 480 at 30 frames per second, Movie Length/Maximum Duration: 29 minutes and 59 seconds, Maximum File Size: 4 GB
Lens: Macro Lens

Computer Requirements

Toshiba Satellite-Laptop, C640-I401A model, Intel Core i3-370M processor, 2GB RAM, and internal storage of 320 GB. Screen size: 14.0 inches.

Vibration Measurement System

Data acquisition: USB powered SIRIUS® MINI, Software: Dewesoft NVH analysis software. Number of axes: 3, Accelerometer Sensors: 13TI-50G-1, Type: IEPE, Sensitivity: 100mV/g Weight: 10 g Frequency range: 2 to 5000 Hz ± 10%, Dimensions: 15.0 × 15 × 15 mm, Temperature Range: -51 degrees to +85 °

 https://doi.org/10.37896/pd91.4/91484

ISSN: 0369-8963

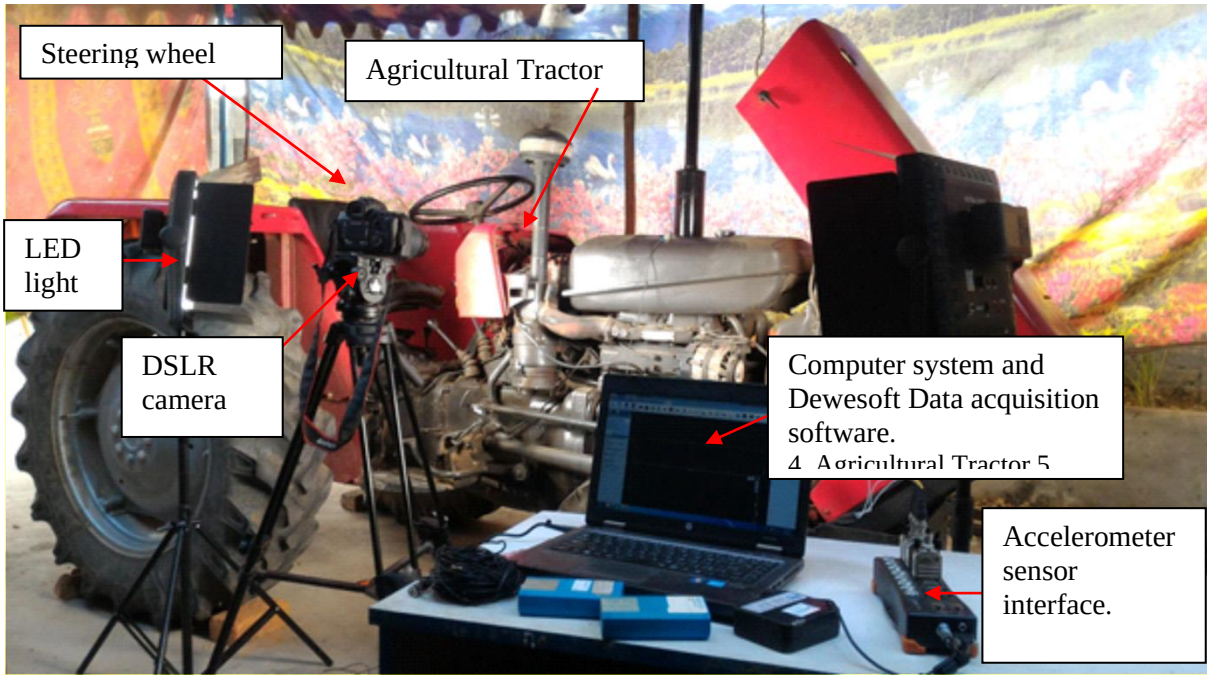

Fig 1: Experimental setup- Overall view

Figure 1 illustrates the test rig, which includes an agriculture tractor, an LED light source with a variable power switch to control the intensity of the light, a DSLR camera, a computer, and an adapter for the accelerometer sensor.

EXPERIMENTAL METHOD

Canon DSLR EOS50 mark II can shoot at 100fps and 30fps with resolutions of 640 x 480 and 1920 x 1080. The left bottom corner of a 640 x 480 pixel video frame measures (0.0, 0.0), while the right top corner measures (640 x 480). A known paper sticker was pasted to the mudguard body, where video was recorded for vibration analysis. The real-world size of the sticker is associated with the image size in pixels, and the image dimensions were set to the real-world dimensions using an appropriate correction factor.

Figures 3 and 4 demonstrate a realistic arrangement of real-world-sized paper stickers. The sticker's length and height were utilised to provide real-world dimensions. The coloured dot on the sticker can be used as a target point, or any point on the sticker can be used as a target point. At least one key-frame is necessary to run the programmed scan in a template matching the displacement. The displacement is calculated with sub-pixel precision via the up-sampled cross-correlation technique. When the sum of squares between the match pixel and the template pixel of RGB contrast is the greatest, the template is matched. [5]

Fig 2: Experimental setup sticker with known dimension

https://doi.org/10.37896/pd91.4/91484

ISSN: 0369-8963

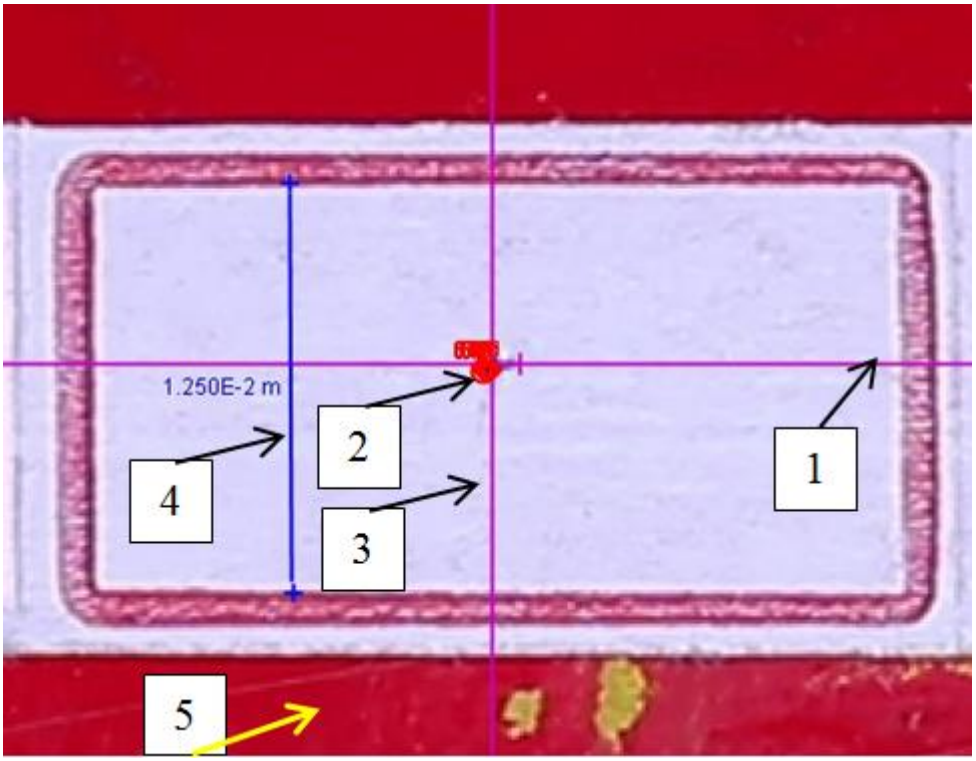

Fig .3 Reference paper stickers on the mudguard

1. X-axis 2. Target point 3.y-axis 4. Real-world reference line 5. Radiator body

RESULTS AND DISCUSSION

Figures 4–11 illustrate the acceleration values produced from the image vision process mathematical technique and measured by the traditional acceleration sensors and Dewesoft interface software. The graph trend reveals that the two measuring procedures agree well.

Figures 5 and 6 compare the vibration amplitude to one second. The greatest positive amplitude is 0.17 sec with a 5% error, while the maximum negative magnitude is 0.96 sec with a 5% error. The largest percentage of errors is recorded at 0.46 sec, 0.58 sec, and 0.92 sec, with errors ranging from 30% to 50% at extremely low vibration amplitudes, which are not required for vibration analysis. The greatest error was reported at very low acceleration values of 0.001–0.005ms-2.

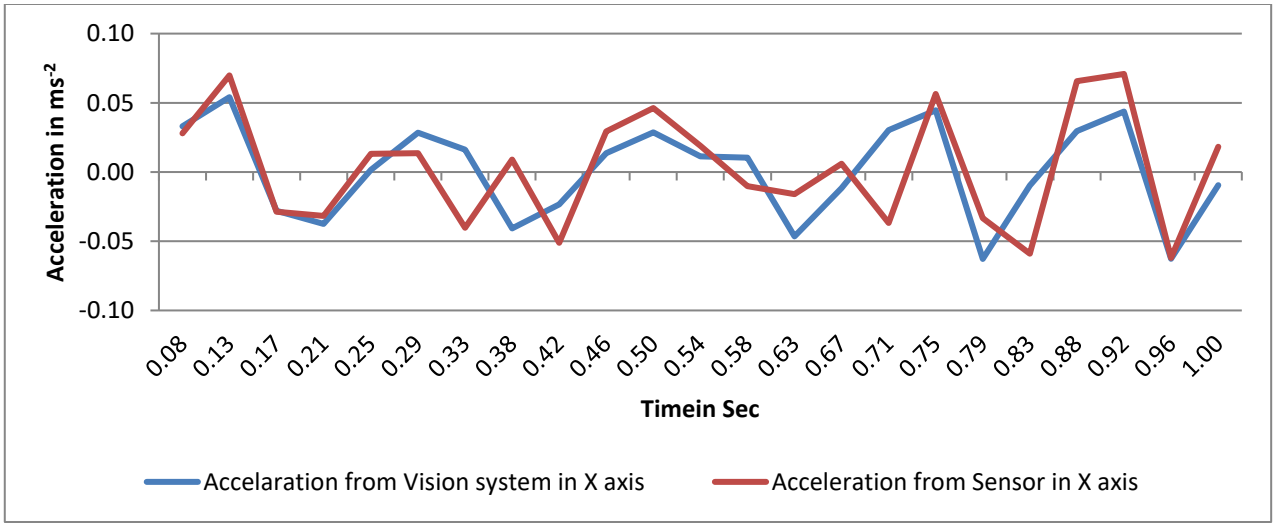

Fig 4 Vibration comparisons for two seconds (0.08 to 1.00 Sec)

https://doi.org/10.37896/pd91.4/91484

ISSN: 0369-8963

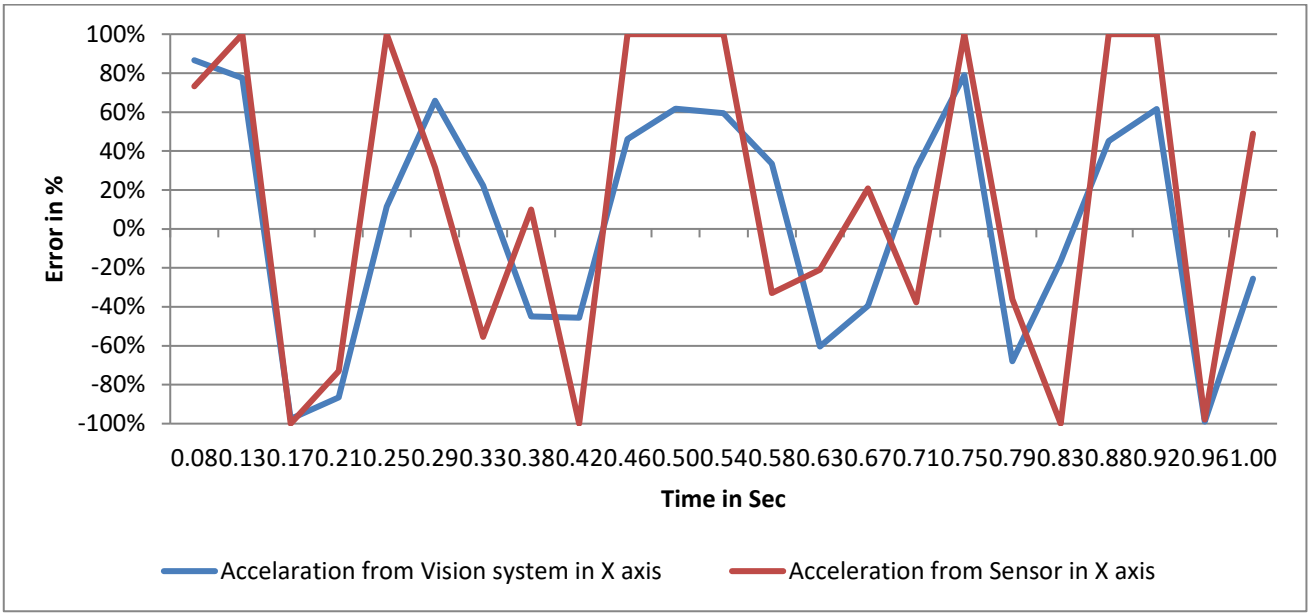

Fig 5 Vibration Error comparisons for two seconds (0.08 to 1.00 Sec)

Figures 7 and 8 compare the vibration amplitude to one seconds. The greatest positive amplitude is 1.25 sec with a 10% error, while the maximum negative magnitude is 1.662 sec with a 10% error. The largest percentage of error is recorded at 1.00 sec, 1.92 sec, and 2.00 sec, with errors ranging from 30% to 50% at extremely low vibration amplitudes, which are not required for vibration analysis. At very low acceleration values of 0.001–0.005ms-2, the greatest error was reported.

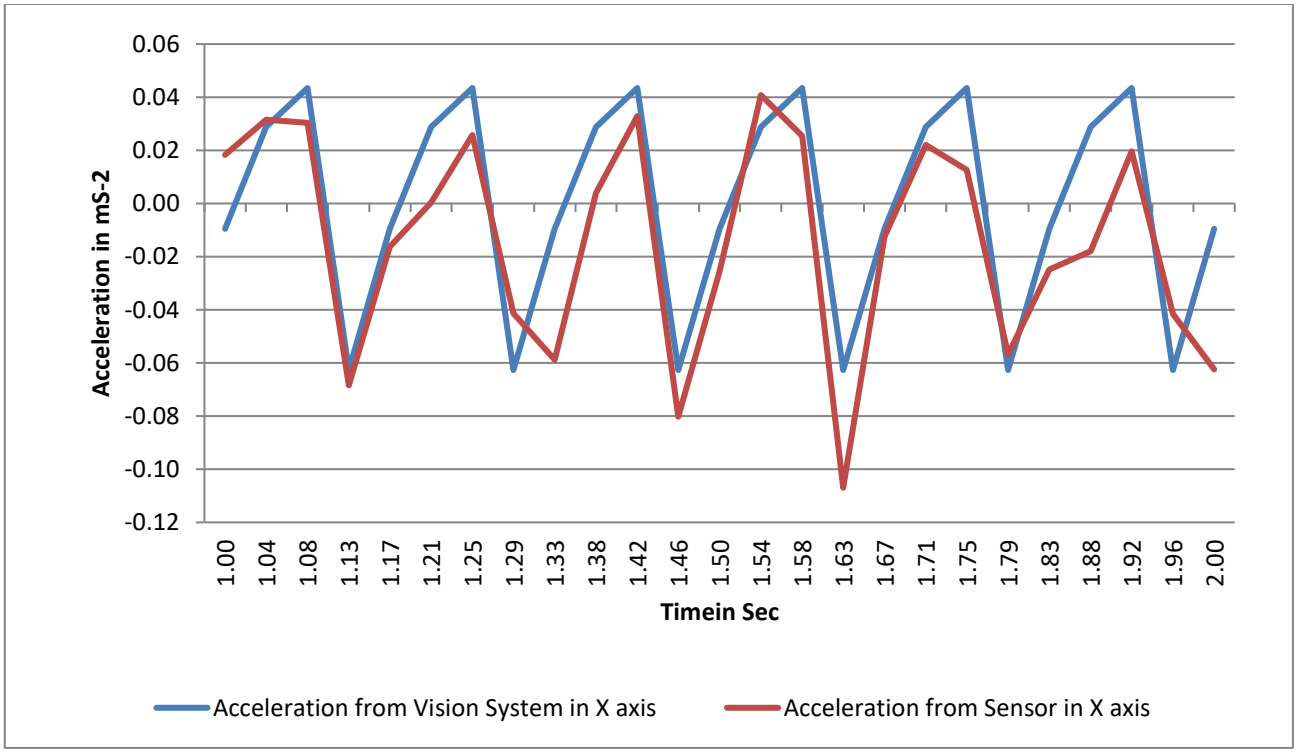

Fig 6 Vibration comparisons for two seconds (1.0 to 2.00 Sec)

https://doi.org/10.37896/pd91.4/91484

ISSN: 0369-8963

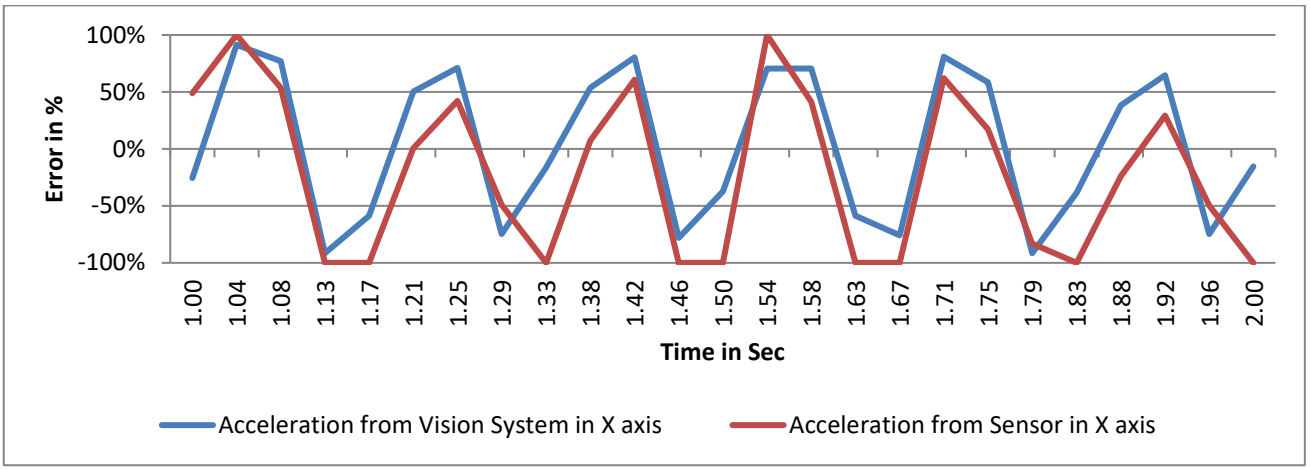

Fig 7 Vibration Error comparisons for two seconds (1.0 to 2.00 Sec)

Figures 6 and 7 compare the vibration amplitude to one seconds. The greatest positive amplitude is 1.25 sec with a 10% error, while the maximum negative magnitude is 1.662 sec with a 10% error. The largest percentage of error is recorded at 1.00 sec, 1.92 sec, and 2.00 sec, with errors ranging from 30% to 50% at extremely low vibration amplitudes, which are not required for vibration analysis. At very low acceleration values of 0.001–0.005ms-2, the greatest error was reported.

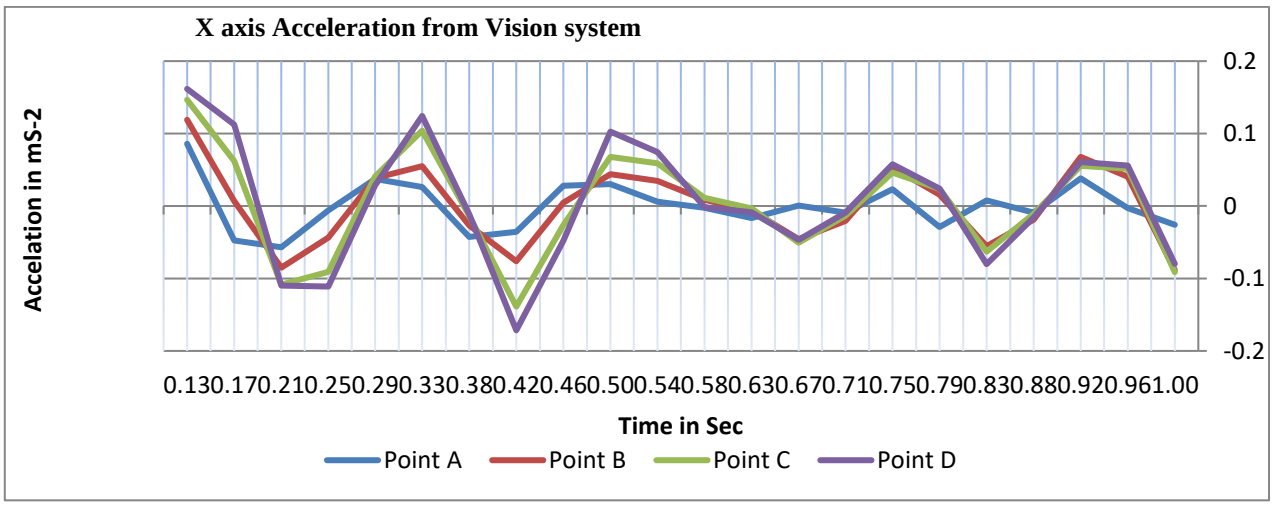

Fig 8 Vibration comparisons for two seconds (0.13 to 1.00 Sec)

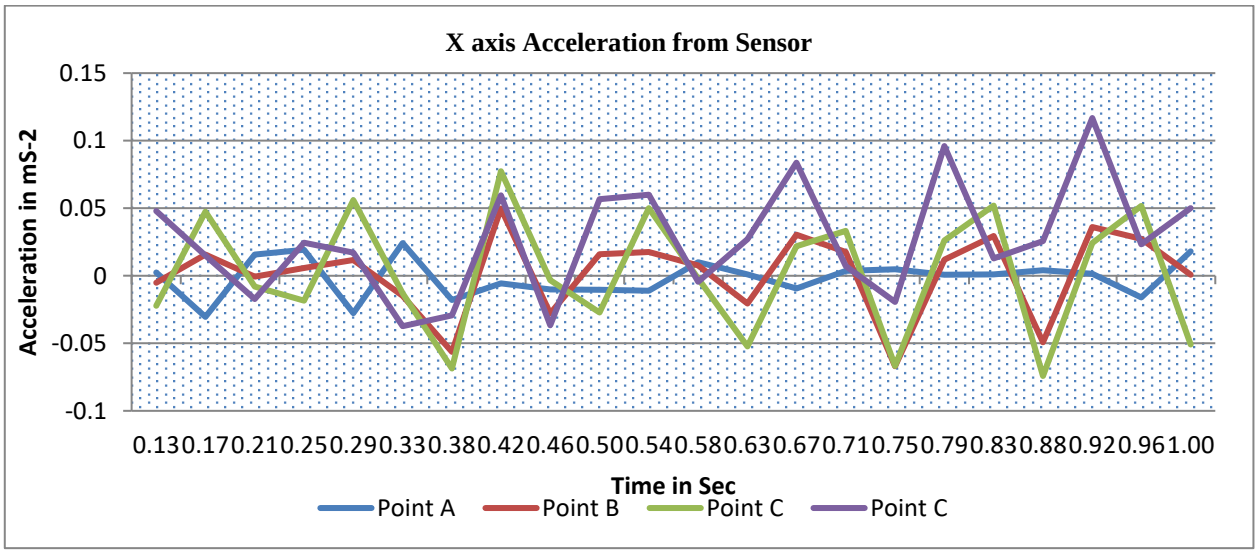

Fig 9 Vibration comparisons for two seconds (0.13 to 1.00 Sec)

https://doi.org/10.37896/pd91.4/91484

ISSN: 0369-8963

Figures 8 and 9 compare the vibration amplitude to one second. It measured the acceleration value in the X axis from the vision system and conventional sensor system at points having little distance between them. Machine vision can measure vibration at that point, while traditional measuring systems seem to be affected by how sensitive the sensors are because they are mounted so closely together.

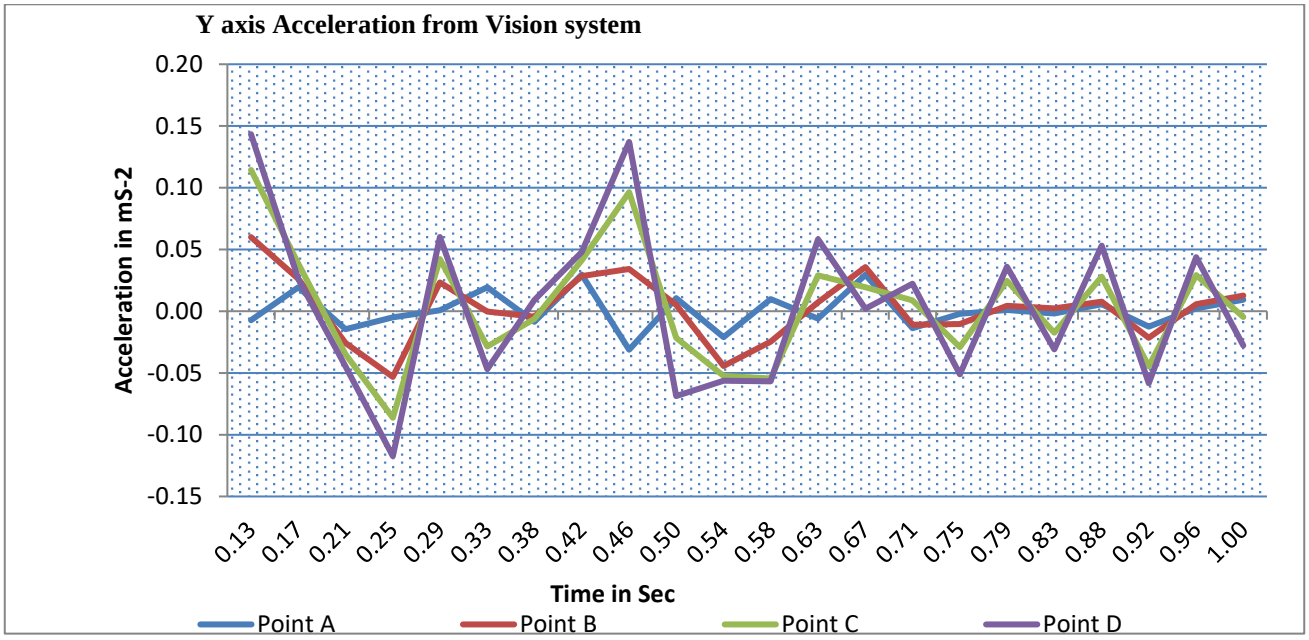

Fig 10 Vibration comparisons for two seconds (0.13 to 1.00 Sec)

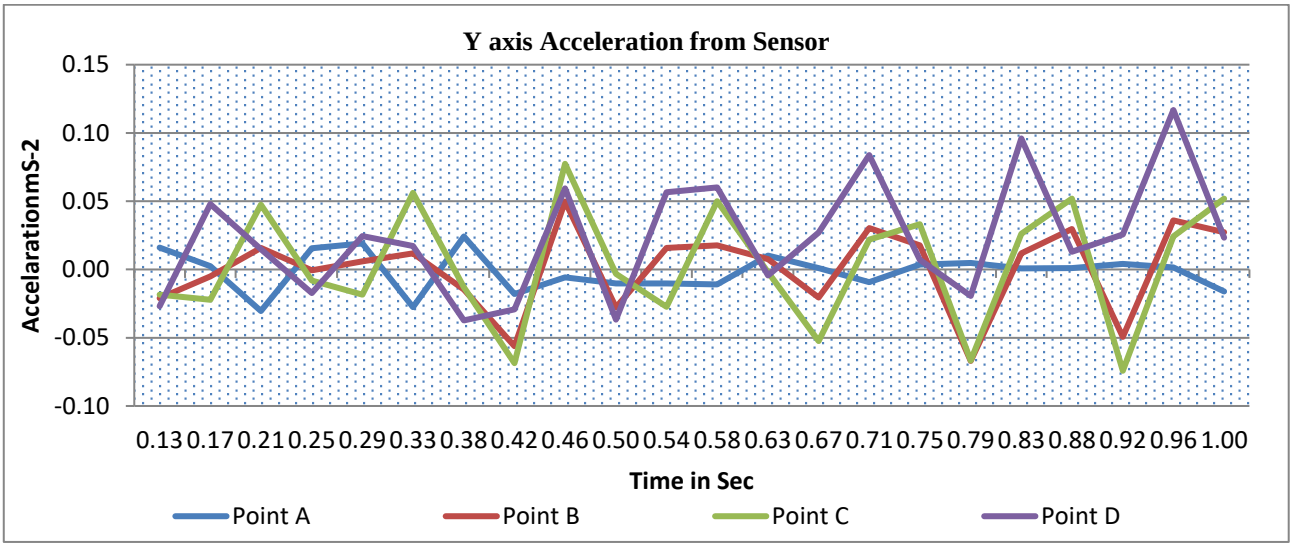

Fig 11 Vibration comparisons for two seconds (0.13 to 1.00 Sec)

Figures 10 and 11 show a comparison of vibration amplitudes to one second displays the acceleration value in the X axis measured by the vision system and the traditional sensor system at very close distances. Traditional measurement methods seem to be affected by sensor sensitivity because the sensors are so close together. Machine vision can measure vibrations in a specific place.

https://doi.org/10.37896/pd91.4/91484

ISSN: 0369-8963

Unlike other evaluation methods in which the precision of the used sensing devices is offered by one‘s manufacturers and normally remains constant within a designated operating condition over a disclosed calibration period, the precision of vision-based systems cannot be purely associated with the functional specifications of the video cameras. The measurement of precision in vision-based monitoring is a complicated subject that requires a multilayered combination and interplay of several criteria. There are three types of sources of mistakes and uncertainty in vision-based monitoring:

(1) Inherent to the monitoring hardware, such as optical distortions and aberrations in the lenses, resolution limitations, and the performance of the video camera's sensor;

(2) related to the software, calibration, and synchronisation process, such as limitations in the motion tracking algorithm, synchronisation lags between cameras, and round-offs in camera calibration; and

(3) Environmental, such as the effect of where the camera is installed and vibrations.

For example, the resolution of the hardware determines how precise the calibration can be, which is controlled by the environment. [25] References [44-48] validated the vision sensor and the proposed vision system. The results and the percentage of inaccuracy were validated by references. The higher the percentage of error, the lower the displacement values; the percentage of error is comparable to the larger value of displacements. The suggested machine vision system has the ability to measure a minimal displacement of 0.01 mm.

CONCLUSION

It has reached the following conclusions:

1. The employment of a macro lens aids in the recording of extremely close picture frames. Close-up pictures give real-world proportions to a white sticker with a precision of 0.01 mm.

2. The percentage of error was measured high at extremely low vibration levels.

3. The suggested probe eliminates the difficulties of camera calibration. Because the image’s dimension is modified with an accuracy of less than one millimeter with a real-world dimension, a white sticker with known real-world dimensions is employed to boost the scaling factor. The white sticker reduces noise in the backdrop image. To conserve time and memory, it conducted image processing without preprocessing the pictures to determine sub-pixel displacements.

4. Different light intensities did not differ substantially in the measuring of vibration levels.

5. The amount of vibration recorded by the machine vision system using the mathematical technique is less than the results of conventional accelerometer readings, which might be attributed to the accelerometer sensor’s sensitivity.

Data availability statement: All data supporting the findings of this study are included within the article (and any supplementary files).

Conflict of interest: The authors declare no competing financial interests or personal relationships that could influence the work reported in this paper.

Funding statement: The funders had no role in the study design, data collection and analysis, decision to publish, or preparation of the manuscript.

 https://doi.org/10.37896/pd91.4/91484

References

[1] S.K. Nithin, K. Hemanth, V. Shamanth, Rayappa Shrinivas Mahale, and P.C. Sharath et al., "Importance of condition monitoring in mechanical domain," *Materials Today: Proceedings*, **2021**, https://doi.org/10.1016/j.matpr.2021.08.299
[2] C-Z. Dong and F .N. Catbas, "A review of computer vision–based structural health monitoring at localand global levels," *Structural Health Monitoring*, vol. 20(2) pp. 692–743, **2021.** DOI: 10.1177/1475921720935585
[3] M. Vishwakarmaa, V. Rajesh Purohitb, P.R. Harshlatac, "Vibration analysis & condition monitoring for rotating machines a review," *Materials Today Proceedings*, vol. 4 pp.2659–2664, **2017**.
[4] M. Kande, A.J. Isaksson, R. Thottappillil, N. Taylor, "Rotating electrical machine condition monitoring automation a review", *J. MDPI*, vol. 5, pp. 24–55, **2017**.
[5] R Ganesan , Dr.G.Sankaranarayanan , Dr.M.Pradeep Kumar and Dr.V.K.Bupesh Raja "Vibration-Based Condition Monitoring of a Tractor Radiator using Machine Vision System", International Journal of Engineering Trends and Technology, vol.70 Issue 1,pp. 283-290, **2022**, doi:10.14445/22315381/IJETT-V70I1P233
[6] KJÆR A/S, Denmark, Website: https://www.bksv.com/en
[7] Y. Xu and J. M. W. Brown john, "Review of machine-vision based methodologies for displacement measurement in civil structures," *Journal of Civil Structural Health Monitoring*, vol, 8 pp. 91–110, **2018**, https://doi.org/10.1007/s13349-017-0261-4
[8] S-W. Kim, N-S, Kim, "Multi-point displacement response measurement of civil infrastructures using digital image processing," *Procedia Engineering*, Volume 14, Pages 195-203, **2011**, https://doi.org/10.1016/j.proeng. 2011.07.023
[9] S. Yoneyama, A. Kitagawa, S. Iwata et al, "Bridge deflection measurement using digital image correlation," *Experimental Techniques*, vol. 31(1), pp. 34 – 40, **2007**, https://doi.org/10.1111/j.1747-1567.2007.00132.x
[10] H. Schreier, J-J. Orteu, MA. Sutton, "Image correlation for shape, motion and deformation measurements: basic concepts, theory and applications," *Springer Science & Business Media*, New York **(2009)** ISBN: 978-0-387-78746-6, DOI:10.1007/978-0-387-78747-3
[11] DV. Jauregui, KR. White, CB. Woodward, KR. Leitch, "Noncontact photogrammetric measurement of vertical bridge deflection," *Journal of Bridge Engineering*, vol. 8, pp. 212–222, **2003**. https://doi.org/10.1061/ (ASCE)1084-0702(2003)8:4(212)
[12] BK. Oh, JW. Hwang, Y. Kim et al, "Vision-based system identification technique for building structures using a motion capture system," *Journal Sound and Vibration*, vol.356 pp.72–85, **2015**. https://doi.org/10.1016/j.jsv.2015.07.011
[13] SW. Park, HS. Park, JH. Kim, H. Adeli, "3D displacement measurement model for health monitoring of structures using a motion capture system," *Measurement*, vol.59, pp. 352–362, **2015.** https://doi.org/10.1016/j.measurement.2014.09.063
[14] B. Pan, K. Qian, H. Xie, A. Asundi , "Two-dimensional digital image correlation for in-plane displacement and strain measurement: a review," *Measurement Science Technology*, vol. 20, pp.62001, **2010**. https://doi.org/10.1088/0957-0233/20/6/062001
[15] MA. Sutton, JH. Yan, V. Tiwari et al. , "The effect of out-of plane motion on 2D and 3D digital image correlation measurements," *Optical Lasers Engineering*, vol. 46, pp. 746–757, **2008**. https://doi.org/10.1016/ j.optlaseng.2008.05.005
[16] RI. Hartley and JL. Mundy, "Relationship between photogrammetry and computer vision. In: Integration photogrammetry techniques with scene analysis and machine vision," *Photogrammetry,SPIE,* vol.1, pp. 92–105, **2008**
[17] R. Jiang, DV, Ja´uregui and KR. White, "Close-range photogrammetry applications in bridge measurement: literature review," *Measurement,* vol. 41, pp. 823–834, **2008**. https://doi.org/10.1016/j.measurement.2007.12.005

[18] G. Moeslund and E. Granum, "A survey of computer visionbased human motion capture," *Computer Vision Image Understanding*, vol. 81, pp. 231–268, **2001**.
[19] H Yoon, H Elanwar, H Choi et al, "Target-free approach for vision-based structural system identification using consumer grade cameras", *Structural Control Health Monitoring*, vol. 23, pp.1405–1416, **2016**. https://doi.org/10.1002/stc.1850
[20] D Ribeiro, R Calcada, J Ferreira and T Martins, "Non-contact measurement of the dynamic displacement of railway bridges using an advanced video-based system," *Engineering Structure*, vol. 75, pp. 164–180, **2014**. https://doi.org/10.1016/j.engstruct.2014.04.051
[21] L-J. Wu, F. Casciati and S. Casciati, "Dynamic testing of a laboratory model via vision-based sensing," *Engineering Structure*, vol. 60, pp. 113–125, **2014**.
https://doi.org/10.1016/j.engstruct.2013.12.002

[22] Xu Yan and M James and W Brown john, " Review of machine-vision based methodologies for displacement measurement in civil structures," *Journal of Civil Structural Health Monitoring*, vol.8 pp.91–110, **2018**, https://doi.org/10.1007/s13349-017-0261-4
[23] P.Kowalski, " Measurements of Vibration Using a High-Speed Camera – Comparative Tests," *Vibrations in Physical Systems*, vol.31, pp1-10, **2020**.
[24] D. Mas, B. Ferrer, P. Acevedo and J. Espinosa, "Methods and algorithms for video-based multipoint frequency measuring and mapping," *Measurement*, **(2016)**,
doi: http://dx.doi.org/10.1016/j.measurement.2016.02.042
[25] Zona, A. "Vision-Based Vibration Monitoring of Structures and Infrastructures: An Overview of Recent Applications," *Infrastructures*, vol.6, pp.4, **2020**,
https://doi.org/10.3390/infrastructures6010004
[26] H. Alkhadafe, A. Al-Habaibeh, S. Daihzong2 and A. Lotfi, "Optimising Sensor Location for an Enhanced GearboxCondition Monitoring System" *Journal of Physics: Conference Series* , vol. 364, pp. 012077, **2012**, doi:10.1088/1742-6596/364/1/012077
[27] Xu Yan, J. Zhang and J. Brown john "An accurate and distraction-free vision-based structural displacement measurement method integrating Siamese network based tracker and correlation-based template matching" *Measurement*, vol.179, pp. 109506, **2021**.
https://doi.org/10.1016/j.measurement.2021.109506
[28] Z. Zhu, Q. Wang, B. Li, W. Wu, J. Yan and et al., "Distractor-aware siamese networks for visual object tracking," *Proc. Eur. Conf. Comput. Vis.*, **2018**, pp. 101–117. https://doi.org/10.1007/978-3-030-01240-3_7.
[29] L. Zhang, A. Gonzalez-Garcia, J. van de Weijer, M. Danelljan, F.S. Khan, "Learning the model update for siamese trackers," *Proc. IEEE Int. Conference Computer Vision*, **2019.**
[30] Bingyou Liu, Pan Yang and Xuan Fan, "High-speed vision measurement of vibration based on an improved ZNSSD template matching algorithm," *Systems Science & Control Engineering*, **2022**, vo. 10:1,pp. 43-54, DOI: 10.1080/21642583.2021.2024099
[31] Kalipada Chatterjee, Venugopal Arumuru, Dhananjay Patil and Rajan Jha "Multipoint monitoring of amplitude, frequency, and phase of vibrations using concatenated modal interferometers," *Scientific Reports*, **(2022)** vol.12, pp. 3798 | https://doi.org/10.1038/s41598-022-07354-6
[32] Ritari, T. et al. "Experimental study of polarization properties of highly birefringent photonic crystal fibers," *Optical Express*, **(2004)**, vol.12, pp. 5931.
[33] Dash, J. N., Jha, R., Villatoro, J. & Dass, S. "Nano-displacement sensor based on photonic crystal fiber modal interferometer," *Optical Letters*, **(2015)**,vol.40, pp. 467.
[34] Barrera, D. et al. "Low-loss photonic crystal fiber interferometers for sensor networks," *J. Light. Technol.*, **(2010)**, 28, 3542–3547.
[35] Pang-jo Chun, Tatsuro Yamane, Shota Izumi and Naoya Kuramoto "Development of a Machine Learning-Based Damage Identification Method Using Multi-Point Simultaneous Acceleration Measurement Results" *Sensors*, **2020,** vol. 20, pp.2780, doi:10.3390/s20102780

[36] Shang, Zhexiong and Shen, Zhigang, "Multi-point Vibration Measurement and Mode Magnification of Civil Structures using Video-based Motion Processing." *Faculty Publications in Construction Engineering & Management*, **(2018)** vol. 23.
[37] S. Geethapriya, K. Devaki, V. Murali Bhaskaran, "Multiple Object Detection in Images using Template Matching," *International Journal of Innovative Technology and Exploring Engineering (IJITEE)*, **2019**, Volume-9 Issue-1, DOI: 10.35940/ijitee.A5187.119119
[38] D.H. Diamond, P.S. Heyns, A.J. Oberholster, "Accuracy evaluation of sub-pixel structural vibration measurements through optical flow analysis of a video sequence," *Measurement*, **2016**, http://dx.doi.org/10.1016/j.measurement. 10.0210263-2241/
[39] Hijazi, A.; Friedl, A.; Kähler, C.J. "Influence of camera's optical axis non-perpendicularity on measurement accuracy of two-dimensional digital image correlation," *Jordan J. Mech. Ind. Eng*. **2011**, 5, Pages 373–382.
[40]. Feng, Dongming, Maria Q. Feng, Ekin Ozer, and Yoshio Fukuda. "A Vision-Based Sensor for Noncontact Structural Displacement Measurement" Sensors 15, no. 7, pp.16557-16575, **2015**. https://doi.org/10.3390/s150716557
[41] Sładek, J.; Ostrowska, K.; Kohut, P.; Holak, K.; Gąska, A. and Uhl, T. "Development of a vision based deflection measurement system and its accuracy assessment," *Measurement* **2013**, vol.46, pp. 1237–1249, 2016
[42] Zhang, Z. " flexible new technique for camera calibration," *IEEE Trans. Pattern Anal. Mach. Intell*.**2000**, vol. 22, Pages 1330–1334.
[43] Dworakowski, Z.; Kohut, P.; Gallina, A., "Holak, K.; Uhl, T. Vision-Based algorithms for damage detection and localization in structural health monitoring," *Struct. Control Health Monit.* **2015**, Volume23, Issue1, , Pages 35-50, doi:10.1002/stc.1755.
[44] Bingyou Liu, Dashan Zhang, Jie Guo, Chang'an Zhu, "Vision-based displacement measurement sensor using modified Taylor approximation approach," *Opt. Eng* **(2016)**, 55(11), Page 114103, doi: 10.1117/1.OE.55.11.114103.
[45] Dongming Feng , Maria Q. Feng, Ekin Ozer and Yoshio Fukuda, "A Vision-Based Sensor for Noncontact Structural Displacement Measurement," *Sensors*, vol. 15(7), pp.16557-16575, **2017**, doi:10.3390/s150716557
[46] Dashan Zhang, Jie Guo, Xiujun Lei and Changan Zhu, "A High-Speed Vision-Based Sensor for Dynamic Vibration Analysis Using Fast MotionExtraction Algorithms," *Sensors*, **2016**, vol. 16, pp. 572; doi:10.3390/s16040572.
[47] Junhwa Lee, Kyoung-Chan Lee, Soojin Cho, and Sung-Han Sim, "Computer Vision-Based Structural Displacement Measurement Robust to Light-Induced Image Degradation for In-Service Bridges," *Sensors* **2017**, vol.17, pp. 2317; doi:10.3390/s17102317
[48] Jaka Javh, Janko Slavic and Miha Boltezar "Measuring full field displacement spectral components using photographs taken with a DSLR camera via an analogue Fourier integral," *Mechanical Systems and Signal Processing*, **2018** , Vol. 100, p. 17-27, DOI: 10.1016/j.ymssp.2017.07.024